

MILITARY TECHNICAL COLLEGE  
CAIRO - EGYPT7<sup>th</sup> INTERNATIONAL CONF. ON  
AEROSPACE SCIENCES &  
AVIATION TECHNOLOGY

## Smart Composite Plate Shape Control Using Piezoelectric Materials I. Finite Element Formulation

M. Adnan Elshafei\*

### ABSTRACT

For the aircraft industry, the ability to change and control the shape of the structure has been a challenging problem. In the current work the shape control of fiber-reinforced composite plate with embedded piezoelectric actuators and sensors is investigated. A finite element formulation is developed for modeling a laminated composite plate, with a distributed piezoelectric actuators and sensors subjected to both mechanical and electrical loads. A simple higher order shear deformation theory with Hamilton's principle is used to formulate the equations of motion. The model is valid for both segmented and continuous piezoelectric elements which can be either surface bonded or embedded in the laminated plate. A four-node, bilinear, isoparametric, rectangular element with seven degrees of freedom at each node is developed. The electric potential is treated as a generalized electric coordinates like the generalized displacement coordinates at the mid-plane of the actuator and sensor layers. The results obtained by the model are compared to the available analytical and the finite element results.

### INTRODUCTION

As a continuous competing requirements for improving the weight, interdisciplinary performance, stability, and reliability of aerospace components, the development of smart composite has generated great interest. Several researchers have studied the interaction between the mechanical properties and the electric field. Crawley et.al [1,2] developed piezoelectric elements for a laminated beams and plates. Lee [3] derived a theory for laminated piezoelectric plates. Wang and Rogers [4] applied the classical laminated plate theory to model laminated plate with spatially distributed actuators. Mitchell and Reddy [5] presented a hybrid theory for enhancing laminated plate based on modeling the electric potential through

---

\* Ph.D., Egyptian Armed Forces

the laminate thickness with 1-D finite element. Ray et. al. [6] presented the exact solutions for a composite plate with piezoelectric actuator and sensor. These solutions however do not provide the results for large complicated structures with integrated materials. Thus, the necessity for approximate techniques such as the finite element method arises. Few papers have been developed addressing the analysis of intelligent structures by the finite element method. Allik and Hughes [7] presented a tetrahedral finite element for a three dimensional electroelasticity. Based on this model, Tzou [8] proposed a method for solving isotropic plate using isoparametric hexahedron solid element and Ha et. al. [9] developed a model for a composite plate by using three dimensional brick element, both elements made the problem complex, costly and required some special techniques to overcome the inaccuracy and disadvantages of modeling a plate with 3-D elements. The two dimensional quadrilateral plate element developed by Hwang et. al [10] is more efficient than solid elements, but it appears to have restricted modeling capabilities. Hwang et. al [11] proposed a model based on classical laminated plate theory which neglects the effects of transverse shear stresses, inadequate for the analysis of moderately thick composite structures. Chandrashekhara et. al. [12] developed a model based on the first order shear deformation theory which need a shear correction coefficients. A static analysis for intelligent plate was presented by Ray [13] using a higher order shear deformation theory which add additional dependent unknowns and make the problem costly to solve. In the present work, a finite element model is developed based on a simple higher order shear deformation theory [14]. The model represents the parabolic distribution of transverse shear stresses and the non-linearity of in-plane displacements across the thickness. The model is able to compute static and dynamic responses of laminated composite plates with distributed piezoelectric actuators and sensors.

### STRAIN-DISPLACEMENT RELATIONS

The displacement field based on a simple higher-order shear deformation theory is given by [14];

$$\begin{aligned}
 U(x, y, z) &= U(x, y, 0) + z\phi_x(x, y, 0) + z^2\zeta_x(x, y, 0) + z^3\zeta_x(x, y, 0) = U_0 + z\phi_{x0} + z^2\zeta_{x0} + z^3\zeta_{x0} \quad (1) \\
 V(x, y, z) &= V(x, y, 0) + z\phi_y(x, y, 0) + z^2\zeta_y(x, y, 0) + z^3\zeta_y(x, y, 0) = V_0 + z\phi_{y0} + z^2\zeta_{y0} + z^3\zeta_{y0} \\
 W(x, y, z) &= W(x, y, 0) = W_0
 \end{aligned}$$

where;  $U_0$ ,  $V_0$  and  $W_0$  are displacements of a point on the reference surface with coordinates  $(x_0, y_0, z_0)$ ,  $\phi_{x0}$  and  $\phi_{y0}$  are the average rotations about y and x axes respectively of the normal to the mid-surface of the undeformed plate.  $z$  is the distance of a point from mid-plane along  $z$  axis. The remaining terms correspond to the higher order rotations. Using the conditions that the top and the bottom surface are free from transverse shear stresses, i.e.  $\tau_{xz}(x, y, \pm t/2) = 0$  and  $\tau_{yz}(x, y, \pm t/2) = 0$ ; where  $t$  is the plate thickness. Therefore the displacement field in equation (1) takes the form;

$$\begin{aligned}
 U(x,y,z) &= U_0 + z \left[ \phi_{x0} - \frac{4}{3} \left( \frac{z}{t} \right)^2 (\phi_{x0} + \partial w / \partial x) \right] \\
 V(x,y,z) &= V_0 + z \left[ \phi_{y0} - \frac{4}{3} \left( \frac{z}{t} \right)^2 (\phi_{y0} + \partial w / \partial y) \right] \\
 W(x,y,z) &= W_0
 \end{aligned}
 \tag{2}$$

By differentiating the displacements in equation (2), the strain can be obtained [15];

$$\begin{aligned}
 \varepsilon_x &= \varepsilon_x^0 + zK_x^1 + z^3K_x^3; & \varepsilon_y &= \varepsilon_y^0 + zK_y^1 + z^3K_y^3; & \varepsilon_{xy} &= \varepsilon_{xy}^0 + zK_{xy}^1 + z^3K_{xy}^3; \\
 \varepsilon_{xx} &= \varepsilon_{xx}^0 + z^2K_{xx}^2; & \text{and} & & \varepsilon_{yz} &= \varepsilon_{yz}^0 + z^2K_{yz}^2
 \end{aligned}
 \tag{3}$$

where;

$$\begin{aligned}
 \varepsilon_x^0 &= U_{0,x}; & \varepsilon_y^0 &= V_{0,y}; & \varepsilon_{xy}^0 &= U_{0,y} + V_{0,x}; & \varepsilon_{xx}^0 &= \phi_{x0} + W_{0,x}; & \varepsilon_{yz}^0 &= \phi_{y0} + W_{0,y}; \\
 K_x^1 &= \phi_{x0,x}; & K_y^1 &= \phi_{y0,y}; & K_{xy}^1 &= \phi_{x0,y} + \phi_{y0,x}; & K_{xx}^2 &= -4(\partial w / \partial x + \phi_{x0}) / t^2; \\
 K_{yz}^2 &= -4(\partial w / \partial y + \phi_{y0}) / t^2; & K_x^3 &= -4(\partial^2 w / \partial x^2 + \phi_{x0,x}) / (3t^2); \\
 K_y^3 &= -4(\partial^2 w / \partial y^2 + \phi_{y0,y}) / (3t^2); & \text{and} & & K_{xy}^3 &= -4(2\partial^2 w / \partial x \partial y + \phi_{x0,y} + \phi_{y0,x}) / 3t^2;
 \end{aligned}
 \tag{4}$$

which include linear strains, curvatures, twists and other higher order curvatures.

### SRESS-STRAIN RELATIONS

For a plane stress approximation since the normal stress  $\sigma_z$  is small it can be neglected, and the corresponding  $\varepsilon_z$  can be eliminated. For fibers oriented at an angle  $\theta$  with the x-axis, the transformed stress-strain relations for a lamina will be

$$\begin{Bmatrix} \sigma_x \\ \sigma_y \\ \sigma_{xy} \\ \sigma_{xx} \\ \sigma_{yz} \end{Bmatrix} = \begin{bmatrix} Q_{11} & Q_{12} & Q_{14} & 0 & 0 \\ Q_{21} & Q_{22} & Q_{24} & 0 & 0 \\ Q_{41} & Q_{42} & Q_{44} & 0 & 0 \\ 0 & 0 & 0 & Q_{55} & Q_{56} \\ 0 & 0 & 0 & Q_{65} & Q_{66} \end{bmatrix} \begin{Bmatrix} \varepsilon_x \\ \varepsilon_y \\ \varepsilon_{xy} \\ \varepsilon_{xx} \\ \varepsilon_{yz} \end{Bmatrix}
 \tag{5}$$

where;

$$\begin{aligned}
 Q_{11} &= C'_{11} \cos^4 \theta + 2(C'_{12} + 2C'_{44}) \cos^2 \theta \sin^2 \theta + C'_{22} \sin^4 \theta \\
 Q_{12} &= (C'_{11} + C'_{22} - 4C'_{44}) \cos^2 \theta \sin^2 \theta + C'_{12} (\cos^4 \theta + \sin^4 \theta) \\
 Q_{14} &= (C'_{11} - 2C'_{44} - C'_{12}) \cos^3 \theta \sin \theta + (C'_{12} - C'_{22} + 2C'_{44}) \cos \theta \sin^3 \theta \\
 Q_{22} &= C'_{11} \sin^4 \theta + 2(C'_{12} + 2C'_{44}) \cos^2 \theta \sin^2 \theta + C'_{22} \cos^4 \theta
 \end{aligned}
 \tag{6}$$

$$\begin{aligned}
 Q_{24} &= (C'_{11} - 2C'_{44} - C'_{12})\cos\theta\sin^3\theta + (C'_{12} - C'_{22} + 2C'_{44})\cos^3\theta\sin\theta \\
 Q_{44} &= (C'_{11} + C'_{22} - 2C'_{44})\cos^2\theta\sin^2\theta + C'_{44}(\cos^4\theta + \sin^4\theta) \\
 Q_{55} &= C'_{55}\cos^2\theta + C'_{66}\sin^2\theta ; \quad Q_{56} = (C'_{55} - C'_{66})\cos\theta\sin\theta \\
 Q_{66} &= C'_{55}\sin^2\theta + C'_{66}\cos^2\theta \\
 \text{And } C'_{ij} &= C_{ij} - C_{i3}C_{j3}/C_{33} \quad \text{for } i,j=1,2,4 \quad \text{and } C'_{ij} = C_{ij} \quad \text{for } i,j=5,6 \quad (7)
 \end{aligned}$$

where  $C_{ij}$  coefficients are the elastic material constants.

### STRESS RESULTANT-STRAIN RELATIONS

Combining equation (3) with equation (5) and integrating layer-by-layer over the thickness, the stress resultants are obtained which can be set in a short form as:

$$\{\bar{R}\} = [\bar{D}]\{\varepsilon^0\} \quad (8)$$

where  $\{\bar{R}\}$  is the stress resultant vector;  $[\bar{D}]$  is the Rigidity matrix which is given in the Appendix, and  $\{\varepsilon^0\}$  is the reference surface strain vector

### PIEZOELECTRIC CONSTITUTIVE RELATIONS

After performing plane stress approximation by setting  $\sigma_z = 0$ , and eliminating the strain  $\varepsilon_z$  the piezoelectric constitutive relations can be written as:

$$\begin{Bmatrix} D_x \\ D_y \\ D_z \end{Bmatrix} = \begin{bmatrix} 0 & 0 & 0 & \bar{e}_{15} & 0 \\ 0 & 0 & \bar{e}_{24} & 0 & 0 \\ \bar{e}_{31} & \bar{e}_{32} & 0 & 0 & 0 \end{bmatrix} \begin{Bmatrix} \varepsilon_x \\ \varepsilon_y \\ \varepsilon_{xy} \\ \varepsilon_{xz} \\ \varepsilon_{yz} \end{Bmatrix} + \begin{bmatrix} \bar{\varepsilon}_{11}^s & 0 & 0 \\ 0 & \bar{\varepsilon}_{22}^s & 0 \\ 0 & 0 & \bar{\varepsilon}_{33}^s \end{bmatrix} \begin{Bmatrix} E_x \\ E_y \\ E_z \end{Bmatrix} \quad (9)$$

$$\begin{Bmatrix} \sigma_x \\ \sigma_y \\ \sigma_{xy} \\ \sigma_{xz} \\ \sigma_{yz} \end{Bmatrix} = \begin{bmatrix} \bar{c}_{11} & \bar{c}_{12} & 0 & 0 & 0 \\ \bar{c}_{21} & \bar{c}_{22} & 0 & 0 & 0 \\ 0 & 0 & \bar{c}_{44} & 0 & 0 \\ 0 & 0 & 0 & \bar{c}_{55} & 0 \\ 0 & 0 & 0 & 0 & \bar{c}_{66} \end{bmatrix} \begin{Bmatrix} \varepsilon_x \\ \varepsilon_y \\ \varepsilon_{xy} \\ \varepsilon_{xz} \\ \varepsilon_{yz} \end{Bmatrix} - \begin{bmatrix} 0 & 0 & \bar{e}_{31} \\ 0 & 0 & \bar{e}_{32} \\ 0 & \bar{e}_{24} & 0 \\ \bar{e}_{15} & 0 & 0 \\ 0 & 0 & 0 \end{bmatrix} \begin{Bmatrix} E_x \\ E_y \\ E_z \end{Bmatrix} \quad (10)$$

where  $\{D\}$  is the electric displacement vector ( $C/m^2$ ),  $\{\varepsilon\}$  strain vector,  $[\varepsilon^s]$  is the dielectric matrix at constant mechanical strain (F/m),  $[E]$  is the electric field vector (V/m),  $\{\sigma\}$  is the stress vector ( $N/m^2$ ) and  $\{c\}$  is the elasticity matrix for a constant electric field ( $N/m^2$ ). And;

$$\bar{e}_{31} = e_{31} - \frac{c_{13}}{c_{33}} e_{33}; \quad \bar{e}_{32} = e_{32} - \frac{c_{23}}{c_{33}} e_{33}; \quad \bar{e}_{24} = e_{24}; \quad \bar{e}_{15} = e_{15}; \quad (11)$$

$$\bar{\epsilon}_{11}^s = \epsilon_{11}^s; \quad \bar{\epsilon}_{22}^s = \epsilon_{22}^s; \quad \text{and} \quad \bar{\epsilon}_{33}^s = \epsilon_{33}^s + \frac{e_{33}^2}{c_{33}}$$

where  $[e]$  is the dielectric permittivity matrix (C/m<sup>2</sup>). The elastic coefficients  $\bar{c}_y$  and  $c_y$  can be obtained by using equation (7).

### VARIATIONAL PRINCIPLE

The Lagrangian  $\mathfrak{I}$  is defined by the summation of kinetic energy and potential energy;

$$\mathfrak{I} = \int_v \left[ \frac{1}{2} \rho \{\dot{q}\}^T \{\dot{q}\} - \frac{1}{2} (\{\epsilon\}^T \{\sigma\} - \{E\}^T \{D\}) \right] dv \quad (12)$$

where;  $\dot{q}$  is the time derivative of the displacement  $q$ ; and  $v$  is the piezoelectric volume. The virtual work done by a surface load  $\{P_s\}$  and the surface charge density  $\mu$  (C/m<sup>2</sup>) applied to the piezoelectric surface areas  $s_1$  and  $s_2$  is;

$$\delta W = \int_{s_1} \{\delta q\}^T \{P_s\} ds_1 - \int_{s_2} \delta \Phi \mu ds_2 \quad (13)$$

where  $\Phi$  is the electric potential (volt). By using Hamilton's principle

$$\int_{t_1}^{t_2} \delta(\mathfrak{I} + W) dt = 0, \quad (14)$$

Since all variations must vanish at  $t = t_1$  and  $t = t_2$ , the variational equation takes the form:

$$\int_v \left[ \rho \{\delta \dot{q}\}^T \{\dot{q}\} + \{\delta \epsilon\}^T [c] \{\epsilon\} - \{\delta \epsilon\}^T [e] \{E\} - \{\delta E\}^T [e]^T \{\epsilon\} - \{\delta E\}^T [\epsilon^s] \{E\} \right] dv - \int_{s_1} \{\delta q\}^T \{P_s\} ds_1 + \int_{s_2} \delta \Phi \mu ds_2 = 0 \quad (15)$$

### FINITE ELEMENT MODELING

A bilinear, isoparametric, rectangular element with four nodes is used. Each node of the element has seven mechanical degrees of freedom. For the element coordinates  $x$  and  $y$ ; in-plane displacements  $U_0$  and  $V_0$  and the two rotations  $\phi_{x0}$  and  $\phi_{y0}$ , the interpolation function is defined as:

$$\Psi = \sum_{i=1}^4 N_i \Psi_i \quad (16)$$

where  $\Psi$  is the value of the variable at any point in the element,  $\Psi_i$  is its value at node point;  $N_i$  is the interpolation function which in the natural coordinate system  $(\xi, \eta)$  is defined by:

$$N_i = 1/4(1 + \xi \xi_i)(1 + \eta \eta_i) \quad (17)$$

where  $\xi$  and  $\eta$  are the local coordinates of the point, and  $\xi_i = -1, 1, 1, -1$  and  $\eta_i = -1, -1, 1, 1$  for  $i = 1, \dots, 4$ . The transverse displacement is interpolated using a non-conforming shape function, which for  $i = 1 \rightarrow 4$  is given by Ziewnkiewicz [16]:

$$\begin{aligned}
 f_i &= (1/8)(1 + \xi\xi)(1 + \eta\eta)(2 + \xi\xi + \eta\eta - \eta^2 - \xi^2) \\
 g_i &= (a/16)\xi(1 + \xi\xi)^2(1 + \eta\eta)(\xi\xi - 1) \\
 h_i &= (b/16)\eta(1 + \eta\eta)^2(1 + \xi\xi)(\eta\eta - 1)
 \end{aligned}
 \tag{18}$$

where  $\xi = 2(x - x_c) / a$ ;  $\eta = 2(y - y_c) / b$ , are the coordinates at the plate center  $(x_c, y_c)$ .

The nodal displacement vector at node  $i$  is defined as:

$$\{q_i\} = [U_{0i} \quad V_{0i} \quad \phi_{0i} \quad \phi_{0i} \quad W_{0i} \quad w_{,xi} \quad w_{,yi}]^T
 \tag{19}$$

The element displacement vector  $\{q_e\}$  is defined as:

$$\{q_e\} = [q_1 \quad q_2 \quad q_3 \quad q_4]^T
 \tag{20}$$

The strain vector at the mid-plane is expressed as:

$$\{\varepsilon^0\} = [B]\{q_e\}
 \tag{21}$$

The matrix  $[B]$  is given in the Appendix, and its elements can be evaluated using the approximation;

$$x = x_c + \xi a/2; \quad y = y_c + \eta b/2
 \tag{22}$$

The generalized strain at a point is related to the reference surface strain as:

$$\varepsilon = [B_1]\{\varepsilon_0\}
 \tag{23}$$

where the matrix  $[B_1]$  is defined in the Appendix. Thus equation (23) can be written as;

$$\varepsilon = [B_1][B]\{q_e\}
 \tag{24}$$

To define the electric field vector  $[E]$ , it is assumed that the electric potential function provides a linear variation across the thickness of the sensor or the actuator layers and gives a zero potential at the interface between the piezoelectric layers and/or the laminated substructure, thus the electric potential function is defined as [13]:

$$\Phi^L(x, y, z) = (z - h_{lp})\Phi_0^L(x, y)
 \tag{25}$$

where  $\Phi_0^L$  can be treated as the generalized electric coordinates like the generalized displacement coordinates at the mid-plane of the actuator and sensor layers. The generalized electric coordinates at any point within the element can then be expressed in terms of  $i$  nodal variable value via interpolation function  $N_\phi$  [17]:

$$\Phi_0^L = [N_\phi]\{\Phi_0^e\}
 \tag{26}$$

where  $\{\Phi_0^e\}$  is the nodal generalized electric coordinate vector and is given by:

$$\{\Phi_0^e\} = [\Phi_{01}^e \quad \Phi_{02}^e \quad \Phi_{03}^e \quad \Phi_{04}^e]^T
 \tag{27}$$

with  $\Phi_{0i}^e$  ( $i=1, \dots, 4$ ) is the generalized electric coordinate at the  $i^{\text{th}}$  node of the element, thus

$$\Phi^L(x, y, z) = (z - h_{lp})[N_\phi]\{\Phi_0^e\}
 \tag{28}$$

where;  $[N_\phi] = [N_1 \ N_2 \ N_3 \ N_4];$  (29)

and  $N_i$  is given in equation (17).

The electric field vector  $\{E\}$  is defined by the electrical potential energy  $\Phi^L$  as:

$$\{E\} = -\nabla \Phi^L \quad (30)$$

By substituting equation (28) in equation (30). Thus;

$$\{E\} = [Z_p][B_\phi]\{\Phi_0^e\} \quad (31)$$

where  $[Z_p]$  and  $[B_\phi]$  are given in the Appendix.

## EQUATIONS OF MOTION

### A. ACTUATOR ONLY

In case of using piezoelectric layers as an actuator only, the system of equations of motion can be obtained by using equations(20), (24) and (31) into the variational equation (15) and adding an artificial linear viscous damping yield the equations of motion in the matrix form:

$$\begin{aligned} [M_e]\{\ddot{q}_e\} + [c_{qq}]\{\dot{q}_e\} + [k_{qq}]\{q_e\} - [k_{q\phi}]\{\Phi_0^e\} &= \{P_M\} \\ [k_{\phi q}]\{q_e\} + [k_{\phi\phi}]\{\Phi_0^e\} &= \{g\} \end{aligned} \quad (32)$$

where

$$[M_e] = \int_V \rho [N]^T [N] dv = \int_A [N]^T [\bar{m}] [N] dA \quad (33)$$

The shape function matrix  $[N]$  and the inertia matrix  $[\bar{m}]$  are given in the Appendix [18], and

$$[k_{qq}] = \int_V [B]^T [B_1]^T [c][B_1][B] dv = \int_A [B]^T [\bar{D}][B] dA \quad (34)$$

where  $[\bar{D}]$  is the rigidity matrix for n layers which is given in the Appendix;

$$[k_{q\phi}] = \int_V [B]^T [B_1]^T [e][Z_p][B_\phi] dv = \int_A [B]^T [BeZ][B_\phi] dA \quad (35)$$

where  $[BeZ]$  for m number of piezoelectric layers is given by:

$$[BeZ] = \sum_{k=1}^m \int_{z_k}^{z_{k+1}} [B_1]^T [e][Z_p] dz; \quad (36)$$

$$[k_{\phi q}] = \int_V [B_\phi]^T [Z_p]^T [e]^T [B_1][B] dv = [k_{q\phi}]^T; \quad (37)$$

$$[k_{\phi\phi}] = \int_V [B_\phi]^T [Z_p]^T [\varepsilon^s][Z_p][B_\phi] dv = \int_A [B_\phi]^T [Z\varepsilon^s Z][B_\phi] dA \quad (38)$$

where  $[Z\varepsilon^s Z]$  for m number of piezoelectric layers is given by:

$$[Z\varepsilon^s Z] = \sum_{k=1}^m \int_{z_k}^{z_{k+1}} [Z_p]^T [\varepsilon^s][Z_p] dz \quad (39)$$

Thus the consistent load vector is;

$$\{P_M\} = \sum_{i=1}^4 \int_{s_1} q_0 \{N_{F_i}\} ds_1 \quad (40)$$

in which  $q_0$  is the intensity of load per unit area, and  $\{N_{F_i}\}$  is the shape function vector at nodal  $i$  given in the Appendix. The electrical excitation  $\{g\}$  is defined as:

$$\{g\} = \int_{s_2} [N_\Phi]^T (z - h_{ip}) \mu ds_2 \quad (41)$$

The charge density on the surface of the actuator layer can be determined as;

$$\mu(x, y) = -\frac{\epsilon_{33}^s}{(z - h_{ip})} \Phi^L(x, y, z) \Big|_{z=h_{op}} \quad (42)$$

where  $h_{op}$ , and  $h_{ip}$  are the distances from structure middle surface to outer and inner surfaces of the piezoelectric actuator layer, respectively. Assembling all the equations gives the global dynamic system equations:

$$\begin{aligned} [M]\{\ddot{q}\} + [C]\{\dot{q}\} + [K_{qq}]\{q\} - [K_{q\Phi}]\{\overline{\Phi}\} &= \{F\} \\ [K_{\Phi q}]\{q\} + [K_{\Phi\Phi}]\{\overline{\Phi}\} &= \{G\} \end{aligned} \quad (43)$$

where  $\{F\}$  is the global mechanical load and  $\{G\}$  is the electrical excitation. In the static case, by performing a condensation of the  $\{\overline{\Phi}\}$  degrees of freedom the static equation of motion can be written as:

$$[K^*]\{q\} = \{F^*\} \quad (44)$$

where

$$\begin{aligned} \{F^*\} &= \{F\} + [K_{q\Phi}][K_{\Phi\Phi}]^{-1}\{G\} \\ [K^*] &= [K_{qq}] + [K_{q\Phi}][K_{\Phi\Phi}]^{-1}[K_{\Phi q}] \end{aligned}$$

and the electrical potential vector is;

$$\{\overline{\Phi}\} = [K_{\Phi\Phi}]^{-1}(\{G\} - [K_{\Phi q}]\{q\}) \quad (45)$$

## B. ACTUATOR AND SENSOR:

When the structure has actuator and sensor layers, after adding an artificial damping and assembling all the equations, the dynamic system equations, can be written as:

$$\begin{aligned} [M]\{\ddot{q}\} + [C]\{\dot{q}\} + [K_{qq}]\{q\} - [K_{q\Phi}]_a \{\overline{\Phi}\}_a - [K_{q\Phi}]_s \{\overline{\Phi}\}_s &= \{F\} \\ [K_{\Phi q}]_a \{q\} + [K_{\Phi\Phi}]_a \{\overline{\Phi}\}_a &= \{G\} \\ [K_{\Phi q}]_s \{q\} + [K_{\Phi\Phi}]_s \{\overline{\Phi}\}_s &= 0 \end{aligned} \quad (46)$$



where  $\{q\}$ ,  $\{\Phi\}_a$ , and  $\{\Phi\}_s$  are the global nodal generalized displacement coordinates, the global nodal generalized electric coordinates for actuator and sensor, respectively. The global nodal generalized electric coordinates can be condensed and the system equations for a static case can be written as:

$$[K^*]\{q\} = \{F^*\} \quad (47)$$

where:

$$\{F^*\} = \{F\} + [K_{q\phi}]_a [K_{\phi\phi}]_a^{-1} \{G\}$$

$$[K^*] = [K_{qq}] + [K_{q\phi}]_a [K_{\phi\phi}]_a^{-1} [K_{\phi q}]_a + [K_{q\phi}]_s [K_{\phi\phi}]_s^{-1} [K_{\phi q}]_s$$

Since the electrical excitation applied to the sensor layer is zero ( $G=0$ ), the voltage from the sensor layer can be written as

$$\{\bar{\Phi}\}_s = -[K_{\phi\phi}]_s^{-1} [K_{\phi q}]_s \{q\} \quad (48)$$

The values of the matrices in equation (46) are computed in the same way as the case (A) of actuator only, (Eq.(43)).

### NUMERICAL INTEGRATION

By using Gauss Legendre quadrature, a full integration technique of 3x3 Gauss points was used to perform the integrations of equations (43) and (46).

### VALIDATION

To demonstrate the performance of the present finite element model, a Matlab code 'CMPZ' was developed. The numerical results were compared to the exact solution [6] and finite element simulation [13]. A square smart plate, consisting of a three-layered (0°/90°/0°) cross-ply laminated plate with the thickness 3 mm was used. A two piezoelectric PVDF layers 40 μm each, served as actuator on the top surface, and a second as sensor on the bottom surface. The elastic properties that simulate a high modulus graphite/epoxy composite are [19]:

$$\begin{aligned} E_{11} &= 172.4 \text{ GPa } (25 \times 10^6 \text{ psi}); & E_{22} &= 6.9 \text{ GPa } (10^6 \text{ psi}); & \nu_{12} &= \nu_{13} = 0.25 \\ G_{12} &= G_{13} = 3.45 \text{ GPa } (0.5 \times 10^6 \text{ psi}); & G_{23} &= 1.38 \text{ GPa } (0.2 \times 10^6 \text{ psi}); \end{aligned}$$

The piezoelectric PVDF layers properties are [8]:

$$\begin{aligned} \text{Dielectric permittivity; } e_{31} &= 0.0460 \text{ C/m}^2, e_{32} = 0.0460 \text{ C/m}^2, e_{33} = 0.0000 \text{ C/m}^2, \text{ and} \\ \text{Dielectricity; } \epsilon_{11}^s &= 0.1062 \times 10^{-9} \text{ F/m}, \epsilon_{22}^s = 0.1062 \times 10^{-9} \text{ F/m}, \epsilon_{33}^s = 0.1062 \times 10^{-9} \text{ F/m.} \\ \nu &= 0.29, \rho = 0.1800 \times 10^4 \text{ kg/m}^3, E = 2 \times 10^4 \text{ N/m}^2. \end{aligned}$$

The mechanical loading is described by;  $q = q_0 \sin(\pi x / a) \sin(\pi y / b)$  where  $q_0$  is the intensity of load per unit area ( $\text{N/m}^2$ ). The electric potential distribution is assumed as a double sinusoidal load with amplitude  $V$  in volts;  $\Phi(x, y, h_{op}) = V \sin(\pi x / a) \sin(\pi y / b)$ ; (the electric potential distribution can be obtained by solving Poisson's or Laplace's equations in case of applied charge or voltage, respectively).

The deflection is normalized as :  $\bar{w} = \frac{100E_T}{q_0\lambda h} w$ ; where  $E_T$  is the transverse Young's modulus of the graphite/epoxy layers  $\lambda$  is the span to the thickness ratio,  $h$  is the structure thickness, and  $q_0 = 10 \text{ N/m}^2$ . Figures 1 to 4 show the numerical results for the analysis.

## CONCLUSION

A finite element formulation is presented as a model for analysis of composite structures with a distributed piezoelectric sensors and actuators. The numerical results generated by the developed code agree very well with the exact solution and other finite element solutions. This verifies that the electric-mechanical coupling matrix is correctly formulated. The method developed is much simpler to formulate and more computationally efficient than models based on solid element. The error of the method is increased by decreasing the span to thickness ratio (i.e. 3 and/or 4), and decreased dramatically for higher span to thickness ratio compared to the exact solution [6]. A Hermite cubic interpolation function was used to approximate the transverse deflection, however, this method does not suffer from the shear correction which is problematic in first order shear deformation theory. The developed displacement model can explain the parabolic distribution of the transverse shear stresses as an advantage over the classical laminated plate theory which neglects the effects of transverse shear stresses. The number of degrees of freedom of the element of the present method is one third of the number of degrees of freedom of the element in the model developed by the higher order shear deformation theory, which, of course, save the computational time. The model can be used subsequently in the stress analysis and dynamic and control of a composite structure with distributed actuators and sensors..

## REFERENCES

- [1] E. F. Crawley and J. de Luis, 'Use of piezoelectric actuators as elements of Intelligent structures', AIAA J., Vol.25, pp1373-1385, 1987.
- [2] E. F. Crawley and K. B. Lazarus, 'Induced strain actuation of isotropic and anisotropic plates', AIAA J., Vol.29, No.6, pp944-951, 1990.
- [3] C. K. Lee, 'Theory of laminated piezoelectric plates for design of distributed sensors/actuators. Part I: Governing equations and reciprocal relationships', J. Acoust. Soc. America, Vol.87(3), pp1144-1158, 1990.
- [4] Bor -Tsuen Wang and Craig A. Rogers, 'Laminated plate theory for spatially distributed induced strain actuators', J. Composite Materials, Vol.25, April 1991.
- [5] J.A. Mitchell and J. N. Reddy, 'A refined hybrid plate theory for composite laminates with piezoelectric laminae', Int. J. Solids Struct., Vol.32, No.16, pp2345-2367, 1995.

- [6] M. C. Ray, R. Bhattacharya, and B. Samanta, 'Exact solution for static analysis of intelligent structures', *AIAA J.*, Vol.31, No.9, Sep.1993.
- [7] Henno Allik and Thomas J. R. Hughes, 'Finite element method for piezoelectric vibration', *Int. J. numer. Meths. Engng.*, Vol.2, pp151-157, 1970.
- [8] H. S. Tzou and C.I. Tseng, 'Distributed piezoelectric sensor/actuator design for dynamic measurement / control of distributed parameter systems: A piezoelectric finite element approach', *J. sound. & vibratio*, Vol.138(1), pp17-34, 1990.
- [9] Sung Kyu Ha, Charles Keilers, and Fu-kuo Chang, 'Finite element analysis of composite structures containing distributed piezoceramic sensors and actuators', *AIAA J.*, Vol.30, No.3, March 1992.
- [10] Woo-seok Hwang and Hyun Chul Park, 'Finite element modeling of piezoelectric sensors and actuators', *AIAA J.*, Vol.31, No.5, May 1993.
- [11] Woo-Seok Hwang, Hyun Chul Park and Woon bong Hwang, 'Vibration control of laminated with piezoelectric sensor/actuator : Finite element formulation and modal analysis', *J. Int. Mater. Syst. & Struct.*, Vol.4, 1993.
- [12] K. Chandrashekhara and A. N. Agarwal, 'Active vibration control of laminated composite plates using piezoelectric devices: A finite element Approach', *J. Int. Mater. Syst. & Struct.*, Vol.4, Oct. 1993.
- [13] M. C. Ray, R. Bhattacharyya and B. Samanta, 'Static analysis of an intelligent structure by the finite element method', *computer & structures*, Vol.52, No. 4, pp617-631, 1994.
- [14] . N. Reddy, 'A simple higher-order theory for laminated composite plates', *J. Appl. Mech.*, Vol.51, pp745-752, 1984.
- [15] A. K. Ghosh and S. S. Dey, ' Simple finite element for the analysis of laminated plates', *comput. & Struct.*, Vol.44, No.3, pp585-596, 1992.
- [16] O. C. Ziewnkiewicz and Y. K. Cheung, 'The finite element method for the analysis of elastic, isotropic and orthotropic slabs', *Proc. Inst. Civil Engrs.*, Vol.28, pp471-488, 1964.
- [17] M. Adnan Elshafei, 'Smart composite plate shape control Using Piezoelectric Materials', Ph.D dissertation, U.S. Naval postgraduate school, Sep. 1996.
- [18] A. K. Gosh and S. S. Dey, ' Free vibration of laminated composite plates : A simple finite element based on higher order theory', *Comput. & Struct.*, Vol.52, No.3, pp397-404, 1994.
- [19] N. J. Pagano, ' Exact solutions for composite laminates in cylindrical bending', *J. Comp. Mater.*, Vol.3 (3), pp398-411, 1969.

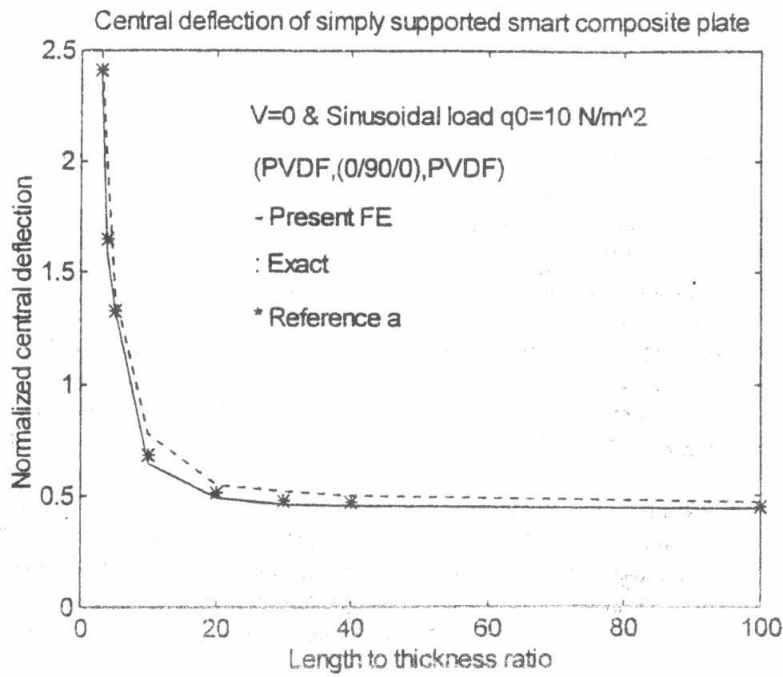


Figure 1: Bending deflection vs. length to thickness ratio for a plate subjected to a double sinusoidal mechanical load.

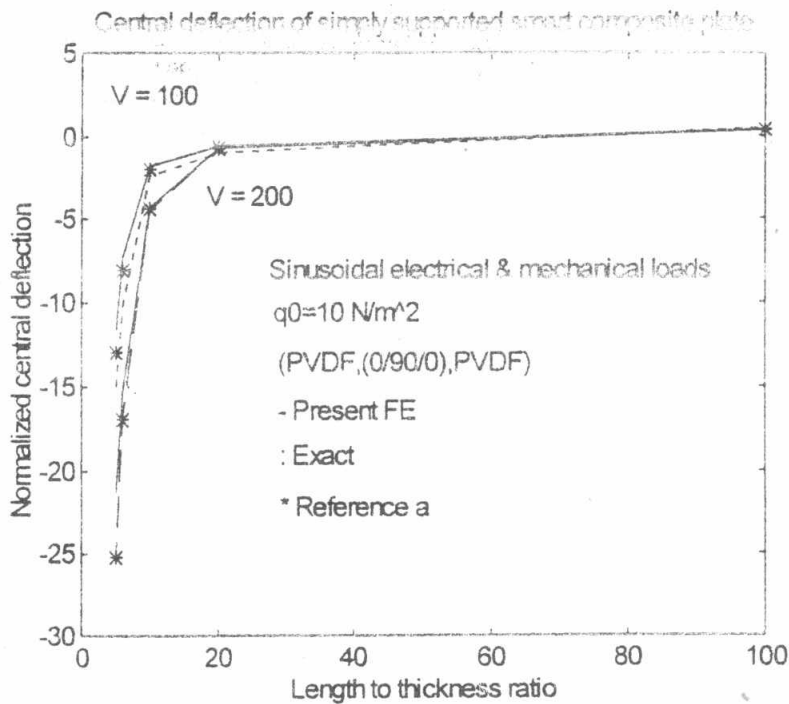


Figure 2: Bending deflection vs. length to thickness ratio for a plate subjected to double sinusoidal electrical and mechanical loads.

Reference a, FE/( Ray, 1994); Exact/(Ray,1993)

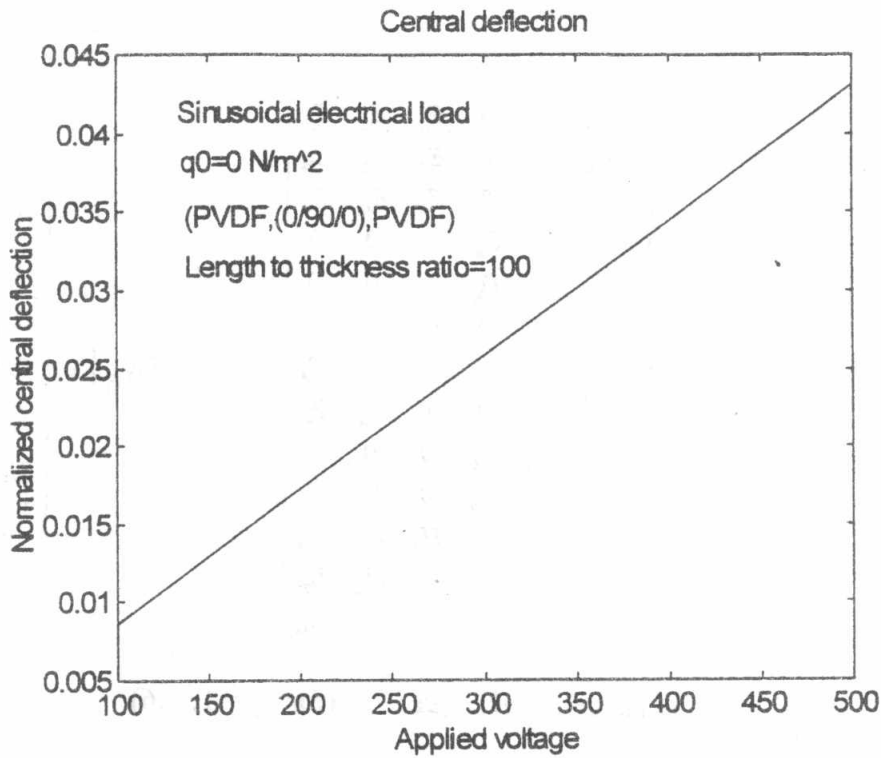


Figure 3: Normalized central deflection vs. applied voltage for a simply supported plate subjected to a uniformly distributed electrical load.

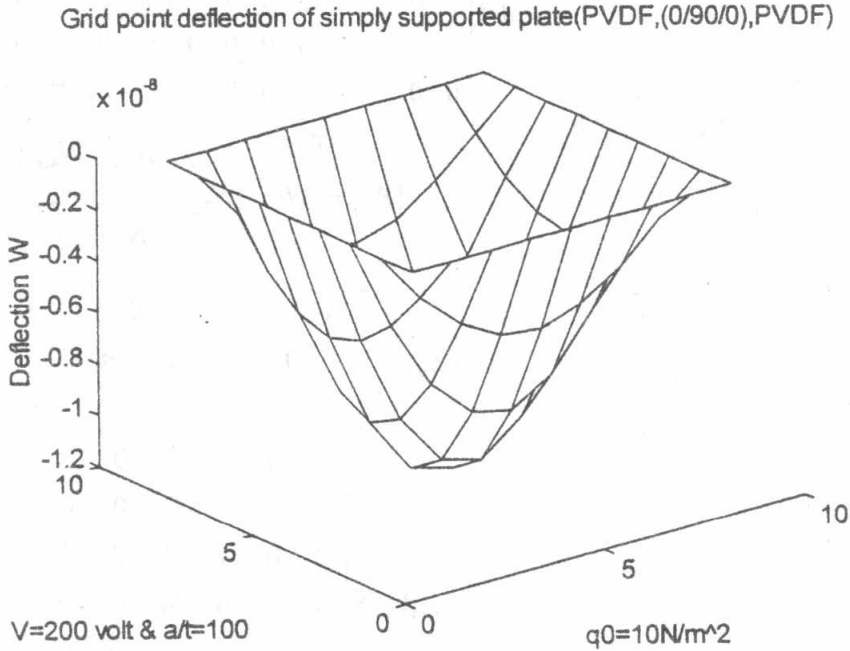


Figure 4: Grid point deflection for simply supported plate subjected to a double sinusoidal electrical and mechanical loads.

Appendix

$$\left[ \begin{array}{cccccccccccc}
 A_{11} & A_{12} & A_{14} & 0 & 0 & B_{11} & B_{12} & B_{14} & 0 & 0 & E_{11} & E_{12} & E_{14} \\
 & A_{22} & A_{24} & 0 & 0 & B_{21} & B_{22} & B_{24} & 0 & 0 & E_{21} & E_{22} & E_{24} \\
 & & A_{44} & 0 & 0 & B_{41} & B_{42} & B_{44} & 0 & 0 & E_{41} & E_{42} & E_{44} \\
 & & & A_{55} & A_{56} & 0 & 0 & 0 & D_{55} & D_{56} & 0 & 0 & 0 \\
 & & & & A_{66} & 0 & 0 & 0 & D_{65} & D_{66} & 0 & 0 & 0 \\
 & & & & & D_{11} & D_{12} & D_{14} & 0 & 0 & F_{11} & F_{12} & F_{14} \\
 & & & & & & D_{22} & D_{24} & 0 & 0 & F_{21} & F_{22} & F_{24} \\
 & & & & & & & D_{44} & 0 & 0 & F_{41} & F_{42} & F_{44} \\
 & & & & & & & & F_{55} & F_{56} & 0 & 0 & 0 \\
 & & & & & & & & & F_{66} & 0 & 0 & 0 \\
 & & & & & & & & & & H_{11} & H_{12} & H_{14} \\
 & & & & & & & & & & & H_{22} & H_{24} \\
 & & & & & & & & & & & & H_{44}
 \end{array} \right]
 \left\{ N_{Fi} \right\} = \begin{bmatrix} 0 \\ 0 \\ 0 \\ 0 \\ f_i \\ g_i \\ h_i \end{bmatrix}$$

Sym.

$$(A_{ij}, B_{ij}, D_{ij}, E_{ij}, F_{ij}, H_{ij}) = \sum_{k=1}^n \int_{z_k}^{z_{k+1}} Q_{ij}(1, z, z^2, z^3, z^4, z^6) dz \quad (\text{for } i, j = 1, \dots, 6)$$

$$\left[ \begin{array}{cccccccc}
 N_{1,x} & & & & & & & \dots \\
 & N_{1,y} & & & & & & \dots \\
 N_{1,y} & N_{1,x} & & & & & & \dots \\
 & & N_1 & f_{1,x} & g_{1,x} & h_{1,x} & & \dots \\
 & & & N_1 & f_{1,y} & g_{1,y} & h_{1,y} & \dots \\
 & N_{1,x} & & & & & & \dots \\
 & & N_{1,y} & & & & & \dots \\
 N_{1,y} & N_{1,x} & & & & & & \dots \\
 & & N_1 & f_{1,x} & g_{1,x} & h_{1,x} & & \dots \\
 & & & N_1 & f_{1,y} & g_{1,y} & h_{1,y} & \dots \\
 N_{1,x} & & & f_{1,x} & g_{1,x} & h_{1,x} & & \dots \\
 & & & & f_{1,y} & g_{1,y} & h_{1,y} & \dots \\
 & & N_{1,y} & f_{1,y} & g_{1,y} & h_{1,y} & & \dots \\
 N_{1,y} & N_{1,x} & 2f_{1,y} & 2g_{1,y} & 2h_{1,y} & & & \dots
 \end{array} \right]
 \left[ B_i \right] = \begin{bmatrix} 1 & 0 & 0 & 0 & 0 & z & 0 & 0 & 0 & 0 & 0 & z^3 & 0 & 0 \\
 0 & 1 & 0 & 0 & 0 & 0 & z & 0 & 0 & 0 & 0 & 0 & z^3 & 0 \\
 0 & 0 & 1 & 0 & 0 & 0 & 0 & z & 0 & 0 & 0 & 0 & 0 & z^3 \\
 0 & 0 & 0 & 1 & 0 & 0 & 0 & 0 & z^2 & 0 & 0 & 0 & 0 & 0 \\
 0 & 0 & 0 & 0 & 1 & 0 & 0 & 0 & 0 & z^2 & 0 & 0 & 0 & 0
 \end{bmatrix}$$

$$\left[ B_\Phi \right] = \begin{bmatrix} N_{1,x} & N_{2,x} & N_{3,x} & N_{4,x} \\
 N_{1,y} & N_{2,y} & N_{3,y} & N_{4,y} \\
 N_1 & N_2 & N_3 & N_4
 \end{bmatrix}$$

$$\left[ Z_p \right] = \begin{bmatrix} -(z-h_p) & 0 & 0 \\
 0 & -(z-h_p) & 0 \\
 0 & 0 & -1
 \end{bmatrix}$$

$$\left[ \bar{m} \right] = \begin{bmatrix} I_1 & 0 & 0 & 0 & 0 & 0 & 0 \\
 0 & I_1 & 0 & 0 & 0 & 0 & 0 \\
 0 & 0 & I_2 & 0 & 0 & 0 & 0 \\
 0 & 0 & 0 & I_2 & 0 & 0 & 0 \\
 0 & 0 & 0 & 0 & I_1 & 0 & 0 \\
 0 & 0 & 0 & 0 & 0 & I_2 & 0 \\
 0 & 0 & 0 & 0 & 0 & 0 & I_2
 \end{bmatrix}$$

$$\left[ N \right] = \sum_{i=1}^4 \begin{bmatrix} N_i & 0 & 0 & 0 & 0 & 0 & 0 \\
 0 & N_i & 0 & 0 & 0 & 0 & 0 \\
 0 & 0 & N_i & 0 & 0 & 0 & 0 \\
 0 & 0 & 0 & N_i & 0 & 0 & 0 \\
 0 & 0 & 0 & 0 & f_i & g_i & h_i \\
 0 & 0 & 0 & 0 & f_{i,x} & g_{i,x} & h_{i,x} \\
 0 & 0 & 0 & 0 & f_{i,y} & g_{i,y} & h_{i,y}
 \end{bmatrix}$$

$$(I_1, I_2) = \sum_{i=1}^n \int_{z_i}^{z_{i+1}} \rho^i [1, z^2] dz \quad \rho^i \text{ is the mass density of the } i \text{ layer.}$$